DOI: https://doi.org/10.57233/ijsgs.v10i1.592 ISSNp: 2488-9229; ISSNe: 3027-1118

IJSGS FUGUSAU VOL10 (1) WEBSITE: https://fugus-ijsgs.com.ng

INTERNATIONAL JOURNAL OF SCIENCE FOR GLOBAL SUSTAINABILITY

(A PUBLICATION OF FACULTY OF SCIENCE, FEDERAL UNIVERSITY GUSAU, NIGERIA)

Ground Magnetic Profiling for Delineating Ore & Marble Deposits Within Okpella, Southern Nigeria

Emenike, K.[1], Aigbedion, I.[1], Akherevebhu, O.[1], Ozegin, K. O.[1], Ataman, O. J.[1], Aigbedion, E.O.[2], and Shaibu I.[3]

[1]Department of Geophysics, Ambrose Alli University, Ekpoma, Edo State, Nigeria.
[2]Offshore Technology Institute, Access and Renewable Engineering, University of Port Harcourt, Nigeria.
[3]Department of Geological Sciences, Federal University Gusau, Zamfara State, Nigeria.

Corresponding Author's Email: isaacaigbedion@yahoo.com

Received on: January, 2024 **Revised and Accepted on:** March 2024 **Published on:** March 2024

ABSTRACT

Ground magnetic profiling was deployed to delineate the occurrences of ore and marble minerals within the study area, Okpella, Edo state, Southern Nigeria. Air borne magnetic survey data (Aeromagnetic) was processed and used to identify zones with magnetic anomalies and obtain the lineament of the area. This was tied to the geological mapping data in order to determine best traverse lines. Ground Magnetic data capturing was conducted in the East-West direction, perpendicular to marble strike direction. Geological and Total magnetic intensity (TMI) maps were generated using Arc GIS and Oasis Montaj software respectively. Structural interpretation of the study area defined twenty two (22) major fault systems, dominantly in the direction, Northeast (NE) - Southwest (SW) and Northwest (NW) – Southeast (SE) as well as minor faults, fractures and folds. Geologic mapping and magnetic survey information defined three (3) geological formations namely; the migmatite gneiss – quartzite (MGQ), granite gneiss (GG), meta-volcanics with mafic intrusive rocks (MVM). Migmatite gneiss- quartzite - Tertiary age Alluvium (MGQ) is characterized with negative magnetic susceptibility ranging from -305.4 nT to -33.4 nT, indicative of destruction of magnetic minerals resulting from the increase in temperature during post orogenic activities. Granite gneiss showed intermediate magnetic susceptibility ranging from -33.5 nT to 85.5 nT, while the meta-volcanic and mafic intrusive (MVM) rock units show high magnetic susceptibility >85.5 nT. Marble deposits targets occurred within granite gneiss - meta-volcanic - mafic intrusive contacts within the study area. The interpreted alteration zones, structures and geology are path finders of marble zones in the migmatite-gneiss-schist-quartzite complex. Marble bodies thickness ranges from 1.63 – 16.2 m for shallow deposits and >16.2 for deeper deposits and an average lateral extent of 20.75 m. It is recommended that core drilling be carried out to validate the findings of the ground geophysical survey.

Keywords: Mignatite gneiss-quartzite, Total magnetic intensity, Igara Schist belt, Marble, Ore

1.0 INTRODUCTION

Okpella lies within the Igara Schist belt in which acid, intermediate and basic igneous rocks are reminiscent of past magmatic activity and possible concomitant metallogenesis (Ogunyele A. C. *et al* 2020). . Like all other schist belts in Nigeria, its meta-volcano sedimentary sequence is geochemically similar to that of meta-volcano sedimentary sequences in ore mineral rich Achaean belts such as Barberton Mountain Land in South Africa, Pilbara belt in Australia and Yellowknife district in Canada (Westall, F. and Hickman-Lewis, K. 2021). In spite of this geochemical attribute that suggest ore mineralization within Okpella and its environs, systematic geo-scientific techniques are yet to be deployed to delineate ore and marble deposits in the area. Presently public interest in Okpella has been focused on marble deposit, which is a major feedstock in the cement industry. Other industrial feed stocks in Okpella include Feldspar, Kaolin, Iron ore and Quartz (Aigbedion and Iyayi, 2007; Olotu *et al* 2022). Ground magnetic profiling has been designed to delineate ore and marble deposits within Okpella area. Magnetism is just like gravity, a potential field. Anomalies in the earth's magnetic field are caused by induced or remnant magnetism. Induced magnetic anomalies are the result of secondary magnetization induced in a ferrous body by the earth's magnetic field. The shape dimensions, and amplitude of an induced magnetic anomaly is a function of the orientation, geometry, size, depth, and magnetic susceptibility of the body as well as the intensity and inclination of the earth's magnetic field in the survey area (Gladman, G. B. *et al* 2021).

The magnetic method is typically used to:

i. locate abandoned steel well casings, buried tanks, pipes and metallic debris.
ii. map old waste sites and landfill boundaries.
iii. map basement faults, basic igneous intrusive and anomalies.
iv. investigate archaeological sites.

DOI: https://doi.org/10.57233/ijsgs.v10i1.592 ISSNp: 2488-9229; ISSNe: 3027-1118
IJSGS FUGUSAU VOL10 (1) WEBSITE: https://fugus-ijsgs.com.ng

The magnetic method involves the measurement of the earth's magnetic field intensity (Arora, K. 2020). Typically the total magnetic field and/or vertical magnetic gradient is measured. Measurements of the horizontal or vertical component or horizontal gradient of the magnetic field may also be made.

1.1 Location of Okpella.

Okpella is located in the northern part of Edo State in Etsako East, along Auchi-Okene expressway. It lies between Latitudes 7 ^{0} 14' 17.80" N to 7^{0} 24' 06.97 " N, and Longitudes 6^{0} 12' 36.60" E to 6^{0} 29' 31.57" E. Figure 1 is the geological map of Okpella indicating the study area.

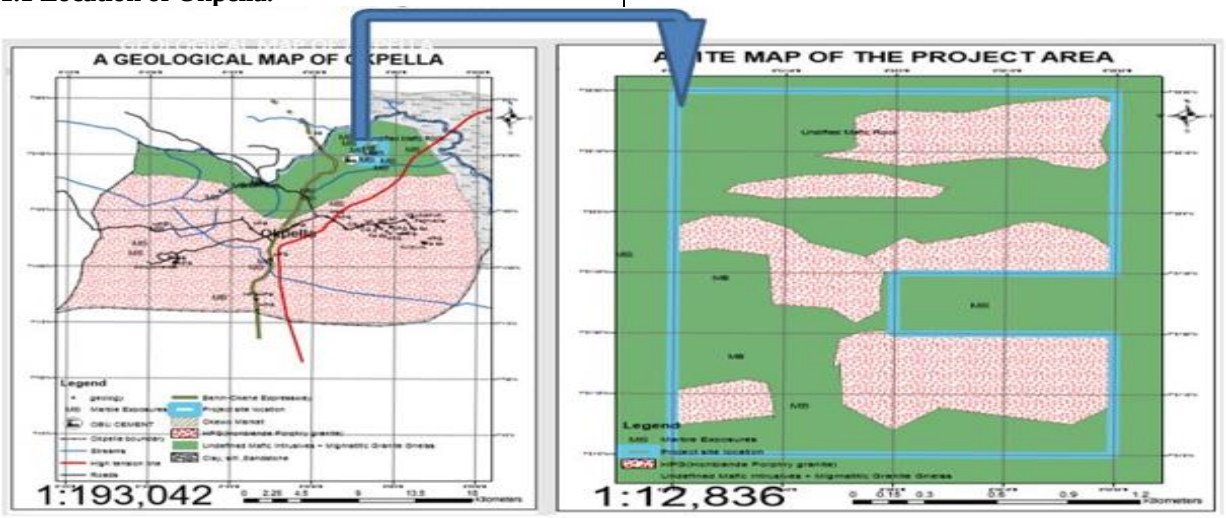

Fig.1: Map of the Study Area

1.2 Geology of Okpella.

Okpella lies within the Igarra schist belt in which acid, intermediate and basic igneous rocks are reminiscent of past magmatic activity and possible concomitant metallogenies. The metasedimentary succession in Okpella formation consists of Quartz biotite Schist, Mica Schist, Marble, Calc-Silicates, and Metaconglomerates. The presence of both calcareous rocks and conglomerates is peculiar to the Schist belts in Nigeria. These rock types together with quartzites occur as bands in the dominant biotite-schists. The gneisses at the margin of the metasediments may be a highly metamorphosed basal part of the sequence. The schist belts represent North-South trending synformal troughs infolded into the migmatite-gneiss complexes which are best developed in the western part of the Country. The schist belts are largely sediment-dominated in contrast to other schist belts of South Africa and Australia. The most important lithologies are pellites, semi-pellites, banded iron formation and quartzite (Turner, 1983; Eludoyin *et al 2023*). This rock suite provides information on the structural pattern of the basement rocks. The contact between the migmatites and the metasediments are fault bounded in most cases (Min J. *et al* 2023), while the schists are presumably a fault-controlled rift like structure (Ogunyele A. C. *et al* 2018).

2.0 MATERIALS AND METHODS

2.1 Materials.

Materials utilized in the research are as follows:

(i) Geological hammer: On the field, hammer was used to chop off sample materials for analysis during ground geological mapping.

(ii) Measuring tape: As an instrument for measuring linear distance, it was used to measure both vertical and horizontal distances during the field operations.

(iii) Geographic positioning system (GPS): Global positioning system set was used to mark traverse points and determine direction of strike and trends of exposed rock bodies. GPS was also used to know the direction and distance of planned site location.

(iv) Compass-clinometer: This was engaged for determining dip and strike of an insitu bodies during filed operations.

(v) Magnet: It was used to confirm the magnetic properties of rock bodies during surface geological mapping.

(vi) Bottle of dilute hydrochloric acid: Dilute HCL was used to confirm the carbonate properties of rock bodies during mapping. The emission of carbon IV oxide indicates the presence of marble or Calc-silicate.

DOI: https://doi.org/10.57233/ijsgs.v10i1.592 ISSNp: 2488-9229; ISSNe: 3027-1118
IJSGS FUGUSAU VOL10 (1) WEBSITE: https://fugus-ijsgs.com.ng

(vii) Marker and masking tape: Makers were used for label writing on the collected samples or label a peg during field operations. Masking tape was used to wrap sample bags and enables indication of codes on it.

(viii) GES's GSM-9 Overhauser magnetometer and accessories: This was the instrument used in measuring magnetic susceptibility anomalies of subsurface rock bodies during ground magnetic profiling operation.

2.2 Softwares

(i) ArcGIS: This was used to interpret and develop surface geological map of the study area.

(ii) Oasis Montaj software: This was used to interpret ground magnetic survey dataset.

2.3 Methods

Surface lithologic mapping was carried out to establish field litho-stratigraphic relationship and associated structures. Geological map was produced on the scale of 1: 193,042 from the field lithologic data. Air borne magnetic survey data (Aeromagnetic data) gotten from Geological Survey Agency of Nigeria was used to identify zones with anomalies. It was processed by carrying out altitude correlation; longitude and latitude correlation was done on the data. The magnetic anomalies were identified and further processing conducted to get the lineament of the area. Areas with lineament were tied to the geological data in order to determine best areas to select traverses. Magnetic data acquisition was conducted along traverses in the neibourhood of igneous intrusions. Areas with high total magnetic field intensity anomalies were identified and interpreted to the possible ore deposits using Oasis Montaj. Such areas were delineated on the produced geological map.

2.4 Survey Design

For a deposit scale survey, the 2.7 km by 2.0 km survey area was mainly demarcated into a 200m traverse lines spacing in order to cover the whole survey area, see Figure 2. The direction of the traverse lines was set out at East -West which is perpendicular to the strike of the anomalous trend determined from the previous geological studies.

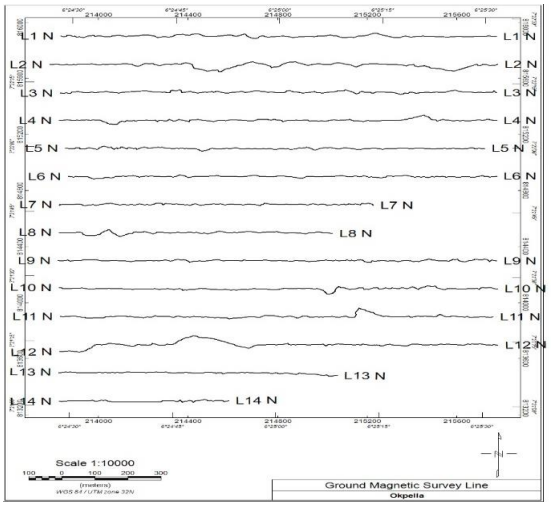

Figure 2: Magnetic Measurements along the E-W traverse lines

2.5 Instrumentation

GEM's GSM-19 Overhauser magnetometer having resolution 0.01 nT and a complete accuracy of 0.2 nT was used for the data acquisition, see figure 3. It consists of a sensor containing a proton-rich fluid. A strong radio frequency is passed through a coil wound around the sensor which polarizes the proton-rich fluid. The proton magnetization is deviated by a short pulse into a plane of precession. A cut in the electrical current causes the polarized protons to proceed in the earth's field and return to steady states after they have decayed slowly. The measured frequency is of the proton precession is converted into units of magnetic field

.

Figure 3: GEM's GSM-19 Overhauser Magnetometer Equipment.

DOI: https://doi.org/10.57233/ijsgs.v10i1.592 ISSNp: 2488-9229; ISSNe: 3027-1118
IJSGS FUGUSAU VOL10 (1) WEBSITE: https://fugus-ijsgs.com.ng

2.6 Field Data Acquisition

Two magnetometers (GSM-19 Overhauser magnetometer) were used which were synchronized during the survey to obtain the lateral variation of magnetic susceptibility of the study area. Within the survey area, one was set up as a continually reading base magnetometer to check the effect of diurnal variations magnetic storms. The other magnetometer (rover) was put in a WALKMAG mode and carried as a backpack so that it continuously records (at sampling rates of up to every 5 second) magnitude of the total magnetic field. In operating the magnetometer during the survey, it was ensured that metallic objects were not carried. Field notebook was carried along to record about any unavoidable magnetic interfering objects. The data was downloaded from the magnetometer and saved after each surveying day.

2.7 Magnetic Data Reduction and Processing

These are quality assurance processes that were used to take out any noise attached to the data that are not associated with the subsurface geology. The following steps below were used to reduce the data to contain information that are relevant to the survey.

2.8 Diurnal Correction

Casual changes in the earth‘s magnetic field were corrected for by finding the difference between the time-synchronized signals measured at the base station magnetometer and the survey data (rover magnetometer). It was assumed that diurnal variation at the base station was same as the survey area.

2.9 Removal of Geomagnetic Reference Field

After correcting for the effect of diurnal variation, the observed magnetic field data was reduced to a residual value by removing the influence of the earth‘s main magnetic field from the survey data. The modelled international geomagnetic reference field for the survey area removed from the observed data was calculated using the IGRF extension in Oasis Montaj software.

2.10 Gridding.

It is very difficult to collect magnetic data in a perfect traverse line and spacing. For a magnetic data in two dimensions, it is imperative to portray the data by finding its values at the various survey points that are evenly spaced at the nodes of grid.

A 40m cell size grid (one – fourth of the traverse line spacing) was created from the residual data (total magnetic intensity) with the help of the minimum curvature method in Gridding extension of the Oasis Montaj software. The gridded data was presented and displayed as an image. Gridding and interpolation of the data permitted the data to be visualized in a continuous form and also allowed image processing and data filtering.

2.11 Post Processing and Enhancement

A number of transformation techniques (liner filtering) are applied to the processed and gridded data (Don H.J.2022). The mathematical enhancement techniques make anomalies less complicated and also allow attributes of a specific interest more pronounced at the expense of others. The filtering process is usually obtained when the Fourier transform of the data is increased in the frequency domain and converting the adjusted dataset back into the space domain and visualized (Don H.J. 2022).

All the filtering and enhancement techniques were automatically applied using the MAGMAP extension of the Oasis Montaj software. The filtering and enhancement techniques applied include Analytical signal and vertical derivatives as described below.

2.12 Analytic Signal

Nabighian suggested the concept of analytic signal (AS) and proposed that in the 2-D case, the horizontal and vertical derivatives of magnetic fields satisfy the Hilbert transform, thus can be regarded as analytic signals. The amplitude of the analytic signal is the same as the total gradient, independent of the direction of magnetization, and represents the envelope of both the vertical and horizontal derivatives over all possible directions of the earth’s field and source magnetization.

$$\frac{\partial \mathrm{T}}{\partial \mathrm{z}} = \mathrm{H}\left[\frac{\partial \mathrm{T}}{\partial \mathrm{x}}\right] \quad (3.1)$$

where;

T = Magnetic anomaly data

H = Hilbert transform

The analytical signal of a real signal f is defined as;

$$\mathrm{AS}\left(\frac{\partial \mathrm{T}}{\partial \mathrm{x}}\right) = \frac{\partial \mathrm{T}}{\partial \mathrm{x}} - \mathrm{iH}\left[\frac{\partial \mathrm{T}}{\partial \mathrm{x}}\right] \quad (3.2)$$

54R

$\mathrm{i} = -1$.

According to the definition, the analytical signal of the potential field obtained by combining these two quantities into a two-dimensional quantity known as the analytic signal is given as;

$$\mathrm{AS}(\mathrm{x},\mathrm{z}) = \frac{\partial \mathrm{T}}{\partial \mathrm{x}} + \mathrm{i}\frac{\partial \mathrm{T}}{\partial \mathrm{z}} \quad (3.3)$$

where:

DOI: https://doi.org/10.57233/ijsgs.v10i1.592 ISSNp: 2488-9229; ISSNe: 3027-1118
IJSGS FUGUSAU VOL10 (1) WEBSITE: https://fugus-ijsgs.com.ng

$\frac{\partial T}{\partial x}$ and $\frac{\partial T}{\partial z} =$ Horizontal and vertical component of the total field respectively,

$T(x,z) =$ Magnitude of the total magnetic field

z and $x =$ Cartesian coordinates for the vertical direction and the direction perpendicular to strike respectively

The amplitude of the analytic signal is defined as;

$$|AS(z)| = \sqrt{\left(\frac{\partial T}{\partial x}\right)^2 + \left(\frac{\partial T}{\partial z}\right)^2} \quad (3.4)$$

The amplitude of the analytic signal is a symmetric bell-shaped function. By examining its profile across a magnetic source, the analytic signal can be used in interpretation to provide an indication of the edges of the causative body. Similarly, for the three-dimensional case, the analytic signal is given by;

$$AS(x,y) = \left(\frac{\partial T}{\partial x}\right) + \left(\frac{\partial T}{\partial y}\right) + \left(i\frac{\partial T}{\partial z}\right) \quad (3.5)$$

where its amplitude is defined as;

$$|AS(x,y)| = \sqrt{\left(\frac{\partial T}{\partial x}\right)^2 + \left(\frac{\partial T}{\partial y}\right)^2 \left(\frac{\partial T}{\partial z}\right)^2} \quad (3.6)$$

The maximum value of the analytic signal determines the edges of a magnetic body.

2.13 First Vertical Derivative.

Derivatives (vertical) are based on the principle that the rates of change of magnetic field are sensitive to rock susceptibilities near the ground surface than at depth. First vertical derivative is physically equivalent to measuring the magnetic field simultaneously at two points vertically above each other, subtracting the data and dividing the result by the vertical spatial separation of the measurement points. The first vertical derivative was obtained from Laplace equation which is used to describe the magnetic potential field (U) thus,

$$\frac{\partial^2 U}{\partial x^2} + \frac{\partial^2 U}{\partial y^2} + \frac{\partial^2 U}{\partial z^2} = 0 \quad (3.7)$$

$$\text{but, } -\text{grad } U = T \quad (3.8)$$

Hence,

$$-\frac{\partial T}{\partial x} - \frac{\partial T}{\partial y} - \frac{\partial T}{\partial z} = 0 \quad (3.9)$$

Therefore,

$$\frac{\partial T}{\partial z} = -\left(\frac{\partial T}{\partial x} + \frac{\partial T}{\partial y}\right) \quad (4.1)$$

where, $U =$ magnetic potential field

$T =$ total magnetic field vector

Rewriting equation (10) in numerical form we have,

$$-\frac{\partial T}{\partial x} = \left[\frac{T(x+\Delta x)-T(x)}{\Delta x} + 0(\Delta x)\right] \quad (4.2)$$

$$0(\Delta x) = \text{error terms} \quad (4.3)$$

$$-\frac{\partial T}{\partial x} = \left[\frac{T(x+\Delta x)-T(x)}{\Delta x}\right] \quad (4.4)$$

Similarly,

$$-\frac{\partial T}{\partial y} = \left[\frac{T(y+\Delta y)-T(y)}{\Delta y}\right] \quad (4.5)$$

Therefore,

$$\frac{\partial T}{\partial z} = -\left[\frac{T(x+\Delta x)-T(x)}{\Delta x}\right] - \left[\frac{T(y+\Delta y)-T(y)}{\Delta y}\right] \quad (4.6)$$

Equation (15) was applied on TMI grid to produce the first derivative map of Figure 5.7.

$$\Delta x = \text{grid interval in x} - \text{direction}$$

$$\Delta y = \text{grid interval in y} - \text{direction}$$

Facilitate the discrimination of close or even superimposed anomalies. This filter also increases the noise level, which limits the use of higher order derivatives (n=2 for example). The vertical derivative is used to delineate the contacts between large-scale magnetic domains because its value is zero over vertical contacts.

3.0 RESULTS AND DISCUSION.

The results from the processed and enhanced magnetic and regional geological map to generate interpretive maps. These maps are interpreted below and thermal alteration zones, structures and geology are then mapped from these maps. The interpreted alteration zones, structures and geology are path finders of marble zones in the migmatite-gneiss-schist-quartzite complex. The zones that have the potential of hosting ore and marble bodies are described here.

3.1 Digital Elevation Map

Digital elevation map reflected the topographic variation of the study area. The dataset was acquired during the ground magnetic survey, and was gridded to produce 2-dimentional and 3-dimentional digital elevation map. Figure 5 is the Digital Elevation Map (DEM) of the study area, it shows that the elevation of the study area ranges from 178 m to 322 m above mean sea level (MSL). The study area has low land in the northern part and high land in the southern part. The highlands trend NNE-SSW with an average height of about 251 m above mean sea level and occupies about half of the study area. The lowland areas depicted by blue colour range from 178 m to 200 m above mean sea level, and are noted to be the valleys of the southern highland. Figure 6 indicates a 3D digital elevation map

DOI: https://doi.org/10.57233/ijsgs.v10i1.592 ISSNp: 2488-9229; ISSNe: 3027-1118
IJSGS FUGUSAU VOL10 (1) WEBSITE: https://fugus-ijsgs.com.ng

which shows the elevation of the study area to be extremely undulating and range.

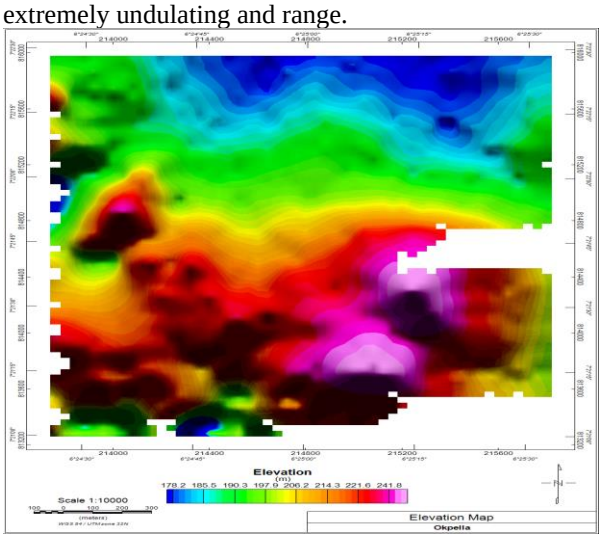

Figure 5: 2-Dimentional Digital Elevation Map of the Study Area.

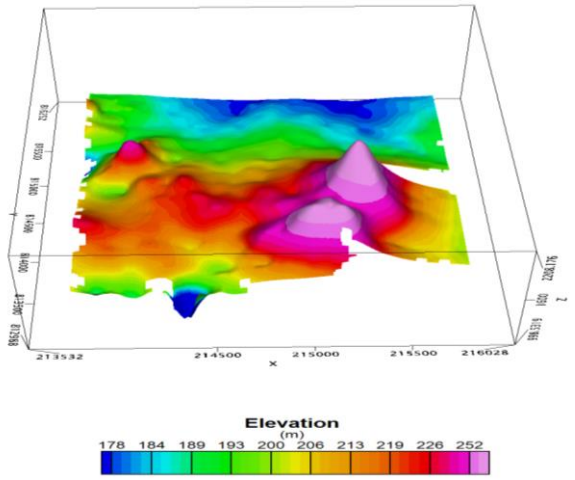

Figure 6: 3-Dimentional Digital Elevation Map of the Study Area.

3.2 Ground Magnetic Interpretation.

Magnetics maps depict the amount of magnetic minerals (magnetite, pyrrhotite) in different rock formations in different colours. The red colour is used to indicate areas with high content of magnetic minerals and the deep blue colour indicates areas with low content of magnetic minerals. Magnetic maps also highlight structures such as folds, faults or shear zones, lithological boundaries between different rock types, and crosscutting.

3.3 Total Magnetic Intensity Map

The Total magnetic intensity map shows the effects of the underlying basement as well as effects of near surface structures within the study area. In the TMI map areas colored blue indicates low magnetic intensity, green indicates intermediate magnetic intensity, and red-pink areas indicate high magnetic intensity, figure 7. This indicates that the area is characterized by high, intermediate, and low amplitude anomalies with magnetic intensities range of ≥ 33280 nT to < 33108 nT. The north part of the study area is characterized by both long and short wavelength (low and high frequency) anomaly bodies with low magnetic magnitude, interpretation of the contour map shows that the signatures trend majorly NE-SW with minor N-S. The southern part of the study area is characterized by short wavelength (high frequency) with high magnetic magnitude bodies and the bodies trends majorly NE-SW with minor NW-SE trend. The southern part of the study area is also characterized by short wavelength (high frequency) bodies that record low magnetic magnitude, they show a major NW-SE trend, with minor NE-SW and N-S trend. The southwestern part of the study area is characterized by long wavelength (low frequency) bodies that has high magnetic magnitude, the body also looks to be trending NE-SW and N-S.

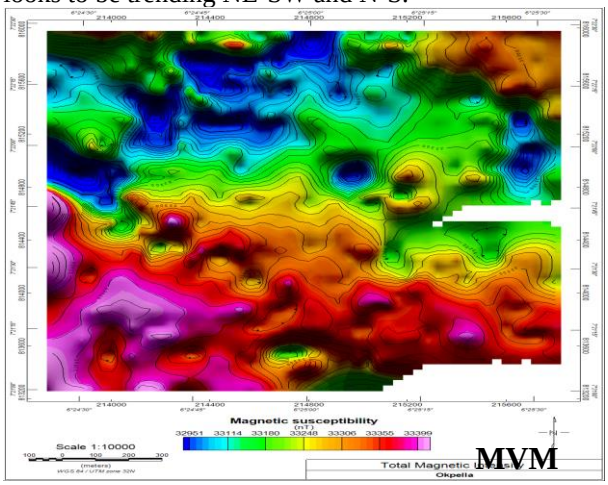

Figure 7: Total Magnetic Intensity Map of the Study Area

The study area is geologically complex, therefore to characterize the magnetic signature to their corresponding geology, topographic constrain is applied to the total magnetic intensity dataset in these was used in the interpretation of the geology, figure 8. The low magnetic susceptibility values (< 33108 nT corresponding to the area with blue colour) observed at the northern parts of the TMI map of the study area falls within low elevation areas (relatively flat lying), this is interpreted as migmatite gneiss- quartzite - Tertiary age Alluvium (MGQ). The intermediate susceptibility values (33108 – 33279 nT, corresponding to the area with green to yellow to red colours) falls within the areas of highest elevation within the study area, it's interpreted as granite gneiss. The highest magnetic susceptibility values (≥ 33280 nT corresponding to the

DOI: https://doi.org/10.57233/ijsgs.v10i1.592 ISSNp: 2488-9229; ISSNe: 3027-1118
IJSGS FUGUSAU VOL10 (1) WEBSITE: https://fugus-ijsgs.com.ng

area with red to pink colour) occurs at the southwestern part of the study area, are interpreted as meta-volcanic and mafic intrusive (MVM), all units are associated with the southwestern basement complex.

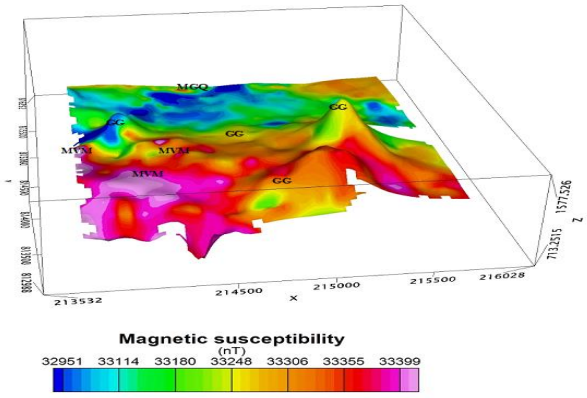

Figure 8: Total Magnetic Intensity Map of the Study Area with Topographic Constrain.

Qualitative interpretation of the total magnetic intensity mapped twenty-two (22) major regional fault within the study area (Figure 9). The faults trend majorly NE-SW and NW-SE. A major fault F1 and F1/ trending NW-SE was defined, the fault is displaced by F9. The NW-SE structures within the study area, is interpreted to have been formed during the formation of the granite gneiss rock unit. F1, F6, F10 and F11 are all associated with the granite gneiss rock unit. Fault F8, F12, F13, F14 and F15 are interpreted as reactivated fault with the migmatite gneiss – quartzite rock unit. The metavolcanics – mafic intrusive of the study area are associated with NE-SW faults and is interpreted to have displaced the NW-SE faults of the granite gneiss rock unit. F2, F3, F4, F5, F7 and F9 are interpreted to be associated with the metavolcanics – mafic intrusive of the study area.

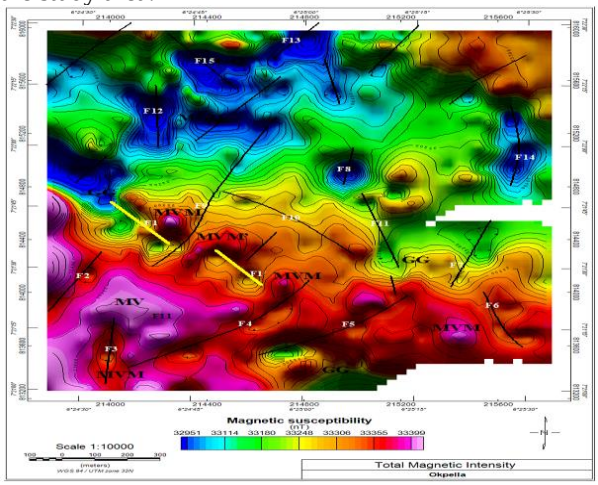

Figure 9: 3-D Total Magnetic Intensity Map of the Study Area

3.4 Regional Residual Separation

In order to emphasize residual anomaly which is of prime interest in mineral exploration, regional-residual separation technique was used to remove the regional constituent, which consist of deep seated bodies from the residual constituent, relating to shallow geological features.

In this case, a linear trend surface is fit into the total magnetic intensity data by a multiple regression technique for the purpose of removing the regional magnetic field. The linear surface so fitted is to remove the regional component of the (TMI) to obtain the residual magnetic anomaly map that would be interpreted.

The residual anomaly map has magnetic amplitude ranging from -305.4 nT to >124.2 nT, see figure 10. Migmatite gneiss- quartzite - Tertiary age Alluvium (MGQ) is characterized by magnetic susceptibility ranging from -305.4 nT to -33.4 nT (blue to green) has notable having negative anomalous signature, granite gneiss is characterized by magnetic susceptibility ranging from -33.5 nT to 85.5 nT, hence indicating moderate accumulation of magnetic minerals. Meta-volcanic and mafic intrusive (MVM) rock units is characterized by magnetic susceptibility >85.5 nT, indicating high magnetic mineral accumulation.

The Migmatite gneiss- quartzite - Tertiary age Alluvium (MGQ) zones within the study area is observed to show high magnetic susceptibility (PIO) are indicative of the potential occurrence of iron ore deposits within the study area. The south-central basement complex is known to host iron ore deposits within the migmatites complex (Ominigbo E. 2022). He described the deposit, as a hematite-magnetite quartz body, and termed it as a ferruginous quartzite. Thereafter, Muecke and Neumann (1985) concluded on mineralogical grounds that the deposit represents a replacement of basement gneisses and amphibolites by iron rich solutions emanating from nearby granitic bodies of the Pan-African Older Granite suite (granite gneiss unit).

DOI: https://doi.org/10.57233/ijsgs.v10i1.592 ISSNp: 2488-9229; ISSNe: 3027-1118
IJSGS FUGUSAU VOL10 (1) WEBSITE: https://fugus-ijsgs.com.ng

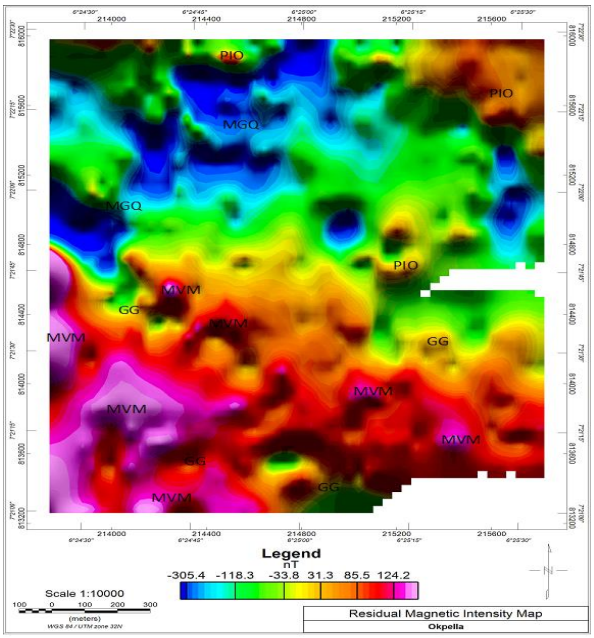

Figure 10: Residual Magnetic Intensity Map of the Study Area.

3.5 Analytical Signal of the Total Magnetic Intensity

The vector nature of magnetic field at low magnetic latitudes places like Nigeria makes the magnetic field (anomalies) developed by magnetized rocks complex and difficult to interpret (Macleod *et al.,* 1993). To position anomalies vertically over the bodies analytical signal filter is applied to the total magnetic field. With this method a maximum anomaly is always produced over the magnetic body regardless of the direction of magnetization of the body (Macleod *et al.,* 1993). Analytic signal transformation is a kind of reduction to the pole from low magnetic latitude. It has an advantage over reduction to the pole and reduction to the equator in that; it is completely independent of the direction of magnetization and the direction of the Earth's field (Don H.J. 2022). This implies that all bodies with the same geometry have the same analytic signal. In addition to this, analytical signal transformations are not subjected to the instability that occurs in reduction to the pole from low magnetic latitudes. The analytic signal maps also define source positions regardless of any remanence in the sources (MacLeod *et al.* 1993). Figure 11 is a map of the analytical signal of the TMI, it is seen from this figure that the high magnetic intensity regions and the low magnetic intensity regions are clearly outlined compared to that seen in the TMI map ,figure 9.

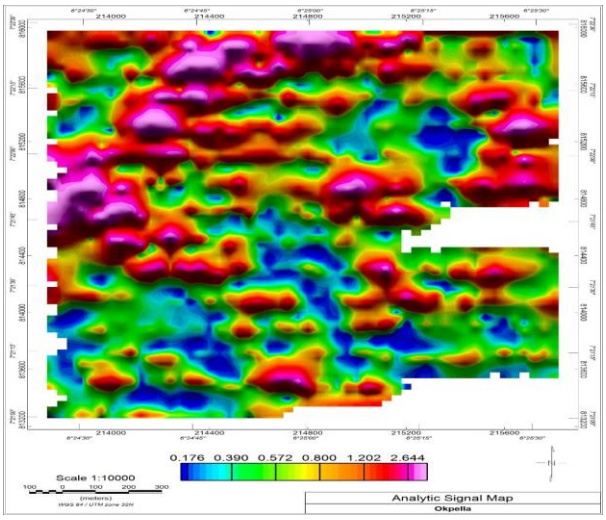

Figure 11: Analytic Signal Map of the Study Area

The analytical signal map has been able to position the anomalies correctly over their causative bodies because the source positions of the anomalies are defined vertically over the source regardless of any remanence in magnetization. In addition, maximum anomaly has been produced over the magnetic body regardless of the direction of magnetization. So, in totality the boundaries that exist for the different geological formations in the study area are well demarcated by the application of the analytical signal. To better the interpretation of the analytic signal map is constrained with the elevation of the study area.From the analytic signal maps shown in figure 11, it is seen that the migmatite gneiss- quartzite - Tertiary ages and Alluvium (MGQ) that occupies the northern part of the study area is observed to have recorded numerous NW-SE and N-S structures, these is interpreted as potential iron ore deposit associated with the quartzite's of the formation. Ominigbo E. 2022 suggested that the iron ore is interbanded with quartzites and is paragenetic with such Precambrian rocks as dolomitic marble, pure marble, phyllite, calc-gneiss, schist and minor intrusive, all of which have been subjected to at least two periods of folding as well as multiple fracturing and sharing. The intermediate magnetic susceptibility of the granite gneiss (GG) rock unit is associated with the thermal action that accompany the mafic intrusions at the southern part the study area. The increase in temperature leads to a destruction of magnetic minerals, therefore recorded low magnetic susceptibility within the granite gneiss was as a result of an increase in temperature resulted in the formation of the marble deposits within the study area. The high magnetic susceptibility within the granite gneiss of the southern part of the study area is interpreted as metavolcanics and mafic intrusive, its strong magnetism arises because of the great production

DOI: https://doi.org/10.57233/ijsgs.v10i1.592 ISSNp: 2488-9229; ISSNe: 3027-1118
IJSGS FUGUSAU VOL10 (1) WEBSITE: https://fugus-ijsgs.com.ng

of secondary magnetite related to amphibole and pyroxene growth during prograde reactions. The low magnetic intensity areas within the granite gneiss (GG) rock unit are of great interest for the identification and mapping of marble bodies.

Marbles occurs within the migmatite-gneiss-schist-quartzite complex as relicts of sedimentary carbonate rocks. These are Upper Proterozoic schist belt metasediments which are normally marked by a general absence of carbonates.

2.6 Vertical Derivative

Computation of the first vertical derivative in a ground magnetic survey is equivalent to observing the vertical gradient directly with a magnetic gradiometer and has the same advantages, namely enhancing shallow sources, suppressing deeper ones, and giving better resolution of closely-spaced sources, Kearey and Brooks, (2002). This helped to better the interpretation of the features f1 to f10 as folds in the derivatives, see figure 12. The fault systems within the study area is also more visible, fault F1 is interpreted to be faulted in two parts, fault F7 and F14 is also well defined. Fault F4 is interpreted to be truncated by intrusive rocks. F8 and F15 structures are interpreted to have been rotated, hence indicating multiple deformation regimes affected the study area.

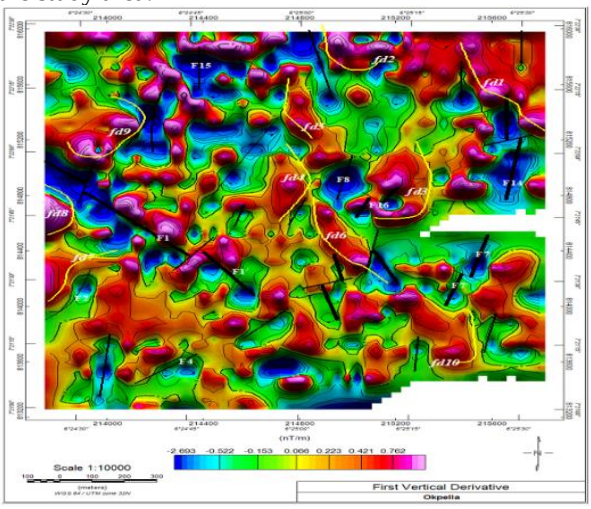

Figure 12: First vertical derivative of Total Magnetic Intensity

Based on the interpretation of the analytic signal map, the marble bodies are interpreted to occur within the low magnetic intensity within the defined granite gneiss rocks. Based on the ground geological information observed around opened pits within the study area, the marble bodies are observed to have been intruded by the mafic rocks (dykes), therefore to separate the zones of mafic intrusion and pure marble bodies, first vertical derivative of the analytic signal was computed. The result of the computation was then compared to the analytic signal map, the first vertical derivative of the total magnetic intensity map, figure 13.Figure 12 is the first vertical derivative of the analytic signal map. For aid interpretation, the known marble pits (MB1, MB2 and MB3) was plotted on the first vertical derivative of the analytic signal map. The first vertical derivative of the analytic signal map was also subjected to topographic constrain to better the interpretation. The zones GGM is interpreted as areas with granite gneiss with mafic intrusive occurrences with no marble deposit, and they are characterized by high analytic signal and first vertical derivative of the analytic signal signature but low first vertical derivative of the total magnetic intensity signature. The marble bodies are characterized by low magnetic signatures within the first vertical derivative of the analytic signal, total magnetic intensity and first vertical derivative of the total magnetic intensity maps. Fault F2 is also better defined, show its NW-SE discontinuity.

DOI: https://doi.org/10.57233/ijsgs.v10i1.592 ISSNp: 2488-9229; ISSNe: 3027-1118
IJSGS FUGUSAU VOL10 (1) WEBSITE: https://fugus-ijsgs.com.ng

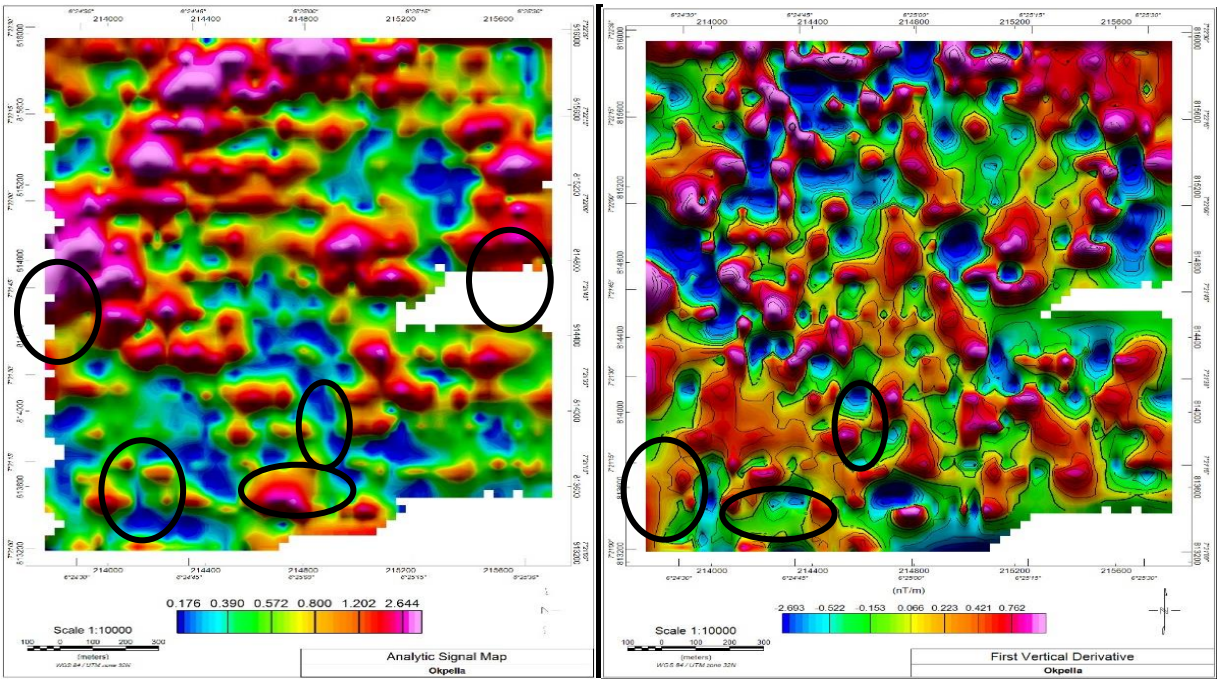

Figure 13: Interpreted Analytic Signal and First Vertical derivative of Total Magnetic Intensity

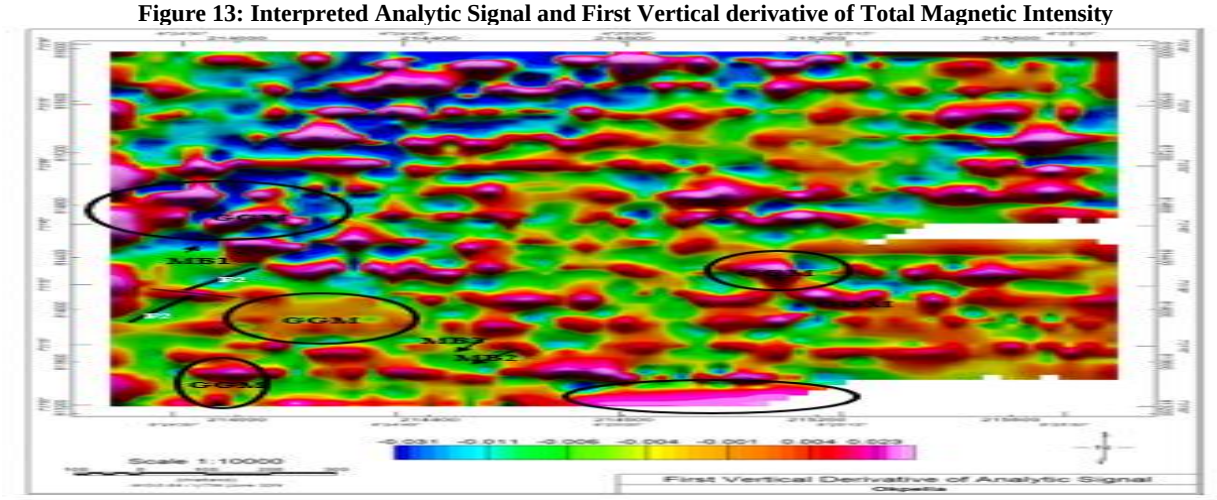

Figure 14: First vertical derivative of the analytical signal

3.7 Interpreted Structural Map

From the magnetic maps shown above, the interpreted structural map of the study area is deduced as shown below in figure 15, it is seen that the study area has a lot of structurally complex features such as major faults that trend northeast and northwest, minor faults, fractures and folds. Precambrian rocks as dolomitic marble, pure marble, phyllite, calc-gneiss, schist and minor intrusive, all of which have been subjected to at least two periods of folding as well as multiple fracturing and sharing (Ominigbo E. 2022); therefore areas with higher structural complexity are likely zones of mineralization (Zlotnikov, 2012). These structures were formed during the deformational stages of the Pan-African orogeny and have served as conduits for rising hydrothermal fluid which contains dissolved minerals. Three deformation events were interpreted from the structure's orientation and cross cutting relationships. The early deformation event is defined to be a ductile deformation producing folds whose axial planes trends N and NE-SW direction, the second deformation event resulted in the reactivation of the D1 structures particularly the folds in the N-S and NW-SE direction and the formation of the major fault systems within the area. The third deformation event produced a transgressive deformation starting with ductile deformation resulting in the development of NE-SW oriented structures, brittle deformation occurring at later

DOI: https://doi.org/10.57233/ijsgs.v10i1.592 ISSNp: 2488-9229; ISSNe: 3027-1118
IJSGS FUGUSAU VOL10 (1) WEBSITE: https://fugus-ijsgs.com.ng

stages of the D3 event producing fractures oriented in the NE-SW and NS direction. These deformation are defined to have resulted from three major orogenic cycles of deformation, metamorphism and remobilization corresponding to the the Eburnean (2,000 Ma), the Kibaran (1,100 Ma), and the Pan-African cycles (600 Ma). The first two cycles were characterized by intense deformation and isoclinal folding accompanied by regional metamorphism, which was further followed by extensive migmatization (Ominigbo E. 2022). The Pan-African deformation was accompanied by a regional metamorphism, migmatization and extensive granitization and gneissification which produced syntectonic granites and homogeneous gneisses (Asubiojo, F. E. *et al* 2022). Late tectonic emplacement of granites and granodiorites and associated contact metamorphism accompanied the end stages of this last deformation. The end of the orogeny was marked by faulting and fracturing (Arlo, B. W. and Adolph, Y. 2023).

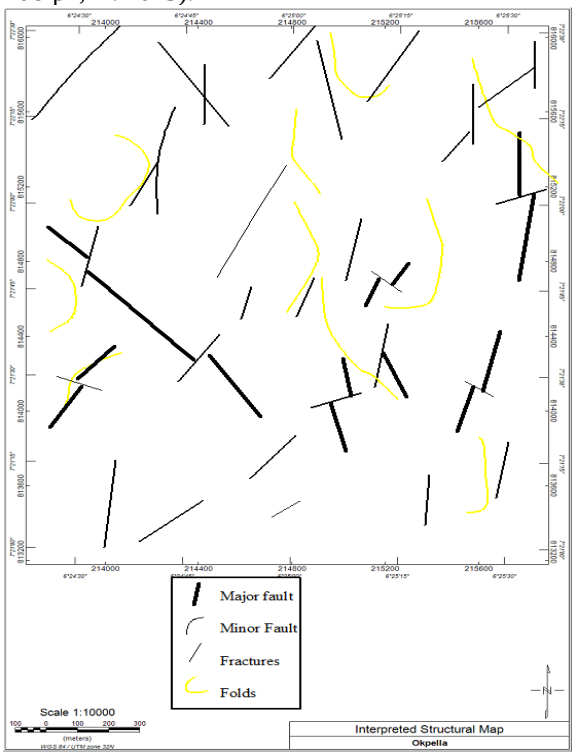

Figure 15: Interpreted structural map of the study area.

3.8 Interpreted Geological Map of Magnetic Data

The interpreted geological map of the surveyed area from the integration of ground magnetic data, surface geologic mapping and topographic information showed that three main geological formations namely the migmatite gneiss- quartzite - Tertiary age Alluvium, granite gneiss and the metavolcanics and mafic intrusive rocks are present in the study area, figure 16. There is observed high susceptibility within the migmatite gneiss- quartzite zone, and it's interpreted as potential iron ore deposit zones as iron ore are usually interbanded with quartzite's and is paragenetic with migmatite gneiss (Precambrian rocks) (Ominigbo E. 2022). The area of marble deposits is defined to occur within granite gneiss rocks that has been mapped and they are closely related to the mafic intrusive of the study area.

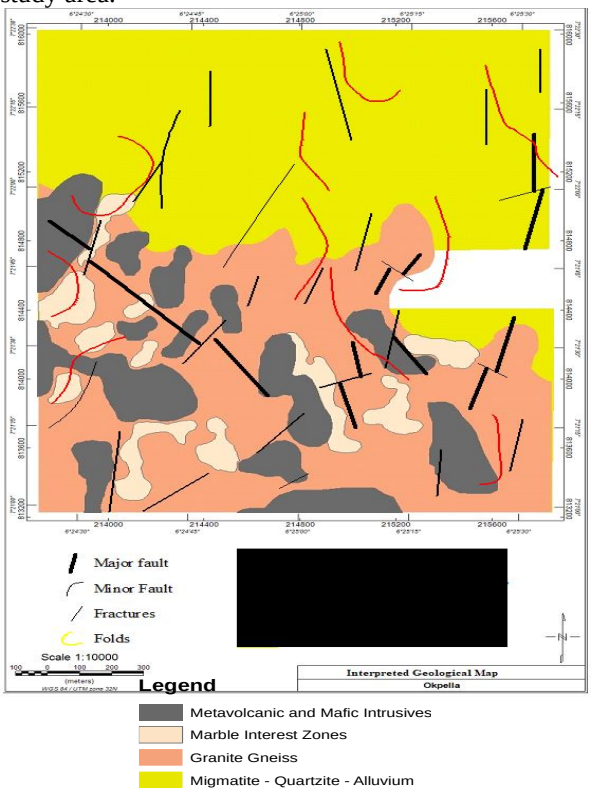

Figure 16: Interpreted Geological Map of the Study Area.

4.0 CONCLUSION

Ground magnetic profiling with the support of surface lithologic mapping and data information gathered from air borne magnetic survey were employed to characterize and interprete surface, subsurface litho-stratigraphy and structural geology with the aim of delineating ore and marble deposits in the study area. Structural interpretation of the study area defined seven (7) major fault systems, as well as minor faults, fractures and folds. The major fault system is dominated by a major NE-SW and NW-SE trend. From the interpretation of the structural maps three deformation events were identified. The early deformation event (D1) is defined to be a ductile deformation producing folds whose axial planes trend N and NE-SW direction, the second deformation event resulted in the reactivation of the D1 structures particularly the folds in the N-S and NW-SE direction and the formation of the

major fault systems within the area. The third deformation event produced a transgressive deformation starting with ductile deformation resulting in the development of NE-SW oriented structures, brittle deformation occurring at later stages of the D3 event producing fractures oriented in the NE-SW and NS direction. These deformations took place in the Eburnean (2,000 Ma), the Kibaran (1,100 Ma), and the Pan-African deformation cycles (600 Ma). Three (3) geological formations were defined, namely the migmatite gneiss - quartzite, granite gneiss, metavolcanics with mafic intrusive rocks. The migmatite gneiss – quartzite complex is characterized by low magnetic intensity with corresponding relatively low elevation, granite gneiss is characterized by intermediate magnetic intensity. Migmatite gneiss-quartzite - Tertiary age Alluvium (MGQ) is characterized by negative magnetic susceptibility ranging from -305.4 nT to -33.4 nT, indicative of destruction of magnetic minerals resulting from the increase in temperature during the Liberian (2,700 Ma), Eburnean (2,000 Ma), the Kibaran (1,100 Ma), and the Pan-African cycles (600 Ma) orogeny that was accompanied by temperature increase. Granite gneiss shows intermediate magnetic susceptibility ranging from -33.5 nT to 85.5 nT, while the meta-volcanic and mafic intrusive (MVM) rock units shows high magnetic susceptibility >85.5 nT. Marble deposits targets occurred within granite gneiss rocks meta-volcanic - mafic intrusive contacts within the study area.

REFERENCES

Aigbedion.I. and Iyayi (2007) Appraisal of Economic importance of Solid Minerals in Ikpeshi and the Environs. A paper presented at the Raw materials Agency, Abuja, and pp. 11-12.

Arora, K. (2020). Magnetic Methods, Principles. In: Gupta, H. (eds) Encyclopedia of Solid Earth Geophysics. Encyclopedia of Earth Sciences Series. Springer, Cham. https://doi.org/10.1007/978-3-030-10475-7_139-1

Asubiojo, F. E and Ayodele, O. S. (2022). Structural geological mapping and mineralization potential indicators in the Psammitic rocks of efon-alaaye and environs, Southwestern Nigeria.

Don H. J. (2022) Investigation of different aspect of filtering in the frequency domain particularly the use of discrete Fourier transforms. Pp 10- 13.

Eludoyin, A. O., Olushola, A., Fashae, O. A., Jeje, L.K.and Faniran, A. (2023). Geology and Landscape of the Southwestern Nigeria. Pp 201 – 216.

Gladman, G. B., Nwankwo, C.N. and Emujakporue, G.O. (2021). Spectral analysis on aeromagnetic data to determine sedimentary thickness over part of Bornu Basin, Northern Nigeria. PP 45 -52.

Kearey, P. and Brooks, M., (2002). An Introduction to Geophysical Exploration. Blackwell Scientific Publications, p. 262.

MacLeod, I.N., Jones, K. and Dai, T.F., (1993), Exploration Geophysics. 3-D analytic signal in the interpretation of total magnetic field data at low magnetic latitudes.

Min J., Xiao-Ying G.and Yong-Fei Z. (2023) The Petrogenetic relationship between Migmatite and Granite in the Himalayan Orogen. Petrological and Geochemical Constraints.

Muecke, A. and Neumann U. (1985) Are the iron ore deposits of Itakpe area of the Itabirite-type or the Itakpeite-type. Abstract, 21st Conference of the Nigerian Mining and Geosciences Society.

Odeyemi, I.B. (1988). Lithostratigraphic and structural relationships of the upper Precambrian metasediments in Igarra area, Western Nigeria. In: Ogezi in the Pre-cambrian Geology of Nigeria. Geological Survey of Nigeria, Kaduna. Pp. 111-123.

Ogunyele, A.C., Obaje, S.O., Akingboye, A.S. et al.(2020). Petrography and geochemistry of Neoproterozoic charnockite–granite association and metasedimentary rocks around Okpella, southwestern Nigeria. Arab J Geosci 13, 780 (2020). https://doi.org/10.1007/s12517-020-05785-x

Ogunyele A. C., Obaje S. O., Akingboye A. S. (2018) Litho-structural Relationships and Petrogenetic Affinities of basement Complex rocks around Okpella, Southwestern, Nigeria.

Arlo,B. W. and Adolph, Y. (2023). The Laramide Orogeny: Current understanding of the structural style, timing and spatial distribution of the classic foreland thick –skinned tectonic system.

Olotu Y., Bada A.O., Elamah D., Akharia O.O. and Erayanmen I.R. (2022) Impact of Limestone Exploitation on the Socio-economic Development of Okpella, Nigeria. DOI: 10.54105/ijee.C1829.051322.

Ominigbo E. (2022) Evolution of the Nigerian Basement Complex, current status and `suggestions for future research. Journal of mining and Geology 58(1) 229 – 236.

Philip Kearey,Michael Brooks and Ian Hill (2002). Introduction to geophysical exploration Pp. 155-163

Turner, D.C., (1983) Upper Proterozoic Schist Belt in the Nigerian Sector of Pan African Province of West Africa.

Westall, F. and Hickman-Lewis, K. (2021). Barberton Greenstone Belt, Traces of Early Life. In: Gargaud, M., et al. Encyclopedia of Astrobiology. Springer, Berlin, Heidelberg. https://doi.org/10.1007/978-3-642-27833-4_150-3

Zlotnikov, D. (2012). Automated Image Analysis Targets Ground Selection; Application of Aeromagnetic Structural Analysis Techniques for Greenfields Gold Exploration.